Chapter 8
Introduction to Organic Vapor Phase Deposition (OVPD®) Technology for Organic (Opto-)electronics

Dietmar Keiper, Nico Meyer, and Michael Heuken

Abstract In this chapter, the organic vapor phase deposition (OVPD®) technology combined with the Close Coupled Showerhead (CCS) technology for the fabrication of sophisticated opto-electronic organic devices based on open literature will be shortly reviewed. Typically, organic (opto-)electronic devices are fabricated by vacuum thermal evaporation (VTE), which is in contrast with the OVPD® technology. The deposition of single organic films, the morphology control by OVPD and the proposed benefits of mixing organic materials, and applying non-sharp interfaces for the overall organic light emitting diode (OLED) performance will be discussed.

8.1 Introduction

The first two-layered organic light emitting diode (OLED) consisting of α-NPD and Alq_3 was reported by Kodak in 1987 [1]. Since that time organic (opto-) electronic devices like Thin Film Transistors (TFTs), solar cells, photo detectors and especially OLEDs for display and solid-state lighting applications have been intensively investigated [2–6]. OLEDs feature beneficial intrinsic properties such as high brightness, low energy consumption, and wide viewing angle characteristics realized in thin devices on glass or on even flexible substrates. This makes them attractive for display application, where they are nowadays applied in cell phones or MP3 players. The next field of commercialization is solid-state lighting [7, 8]. Here, OLEDs reveal additional benefits as area light source with flexible form factors in different colors ranging from red to blue or color mixtures like white light. Latest works on white emitting OLEDs significantly extended the external quantum

M. Heuken (✉) · D. Keiper · N. Meyer
AIXTRON AG, Kaiserstr. 98, 52134 Herzogenrath, Germany
e-mail: D.Keiper@aixtron.com

S. Logothetidis (ed.), *Nanostructured Materials and Their Applications*, NanoScience and Technology, DOI 10.1007/978-3-642-22227-6_8,
© Springer-Verlag Berlin Heidelberg 2012

efficiency (EQE) and efficacies of 102 lm/W (CIE: 0.41; 0.46) [9, 10] and even 124 lm/W (CIE: 0.45; 0.47) were reported using sophisticated organic materials, multilayer OLED stack designs together with improved light outcoupling (ILO) structures [11]. These high efficacies could only be achieved by a sophisticated, ILO approach. Despite the fact that the CIE coordinates are not on the Planckian locus these results prove the potential of OLEDs for solid-state lighting. But beside the efficacy also other, maybe interacting, aspects like lifetime, color, internal quantum efficiency, uniformity, and reproducibility need to be addressed. This needs further improvements on the applied organic materials and on the overall OLED design and fabrication.

The above described record OLED stack applied a layer structure with sharp interfaces and mixtures of in maximum two organic materials [11]. However, other OLED structures were suggested like using three organic materials in one layer and different improvements on the overall OLED were observed [12–14]. One group attributed the improvement of the OLED stack to the fact that the hole transport in the emissive layer (EML) was improved by shifting it from the dopant to the co-dopant. The latter has a lower HOMO than the dopant [9, 13]. By the latter approach a quasi ideal host with perfect HOMO and LUMO levels was created by the combination of a Host, for the electron transport, and an additional second dopant for the hole transport.

Beside the use of more than two different organic molecules in one layer, also a continuously graded transition between the different layers could improve the OLED performance and lifetime, as reported by Kido [15]. Thus, mixing of more than two organic materials and none sharp interfaces offer options to improve the overall OLED performance. Obviously, also other (opto-)electronic organic devices like OTFTs or organic photovoltaic (OPV) could benefit from such approaches.

Typically, these organic devices are fabricated by vacuum thermal evaporation (VTE) technology at chamber pressures of approximately 10^{-6} mbar where the organic material is heated in a source, e.g., crucible, and the organic vapor is deposited on the opposite positioned substrate. Due to the geometrical arrangement of evaporation source and substrate in the same chamber the deposition of material mixtures or concentration gradients with high uniformity on the substrate is limited. In contrast, using the organic vapor phase deposition (OVPD®) technology organic films with material mixtures or even complex concentration variations can be deposited with high homogeneity on the substrate. A detailed comparison of the OVPD® technology with the VTE technology is given elsewhere [16, 17].

In the following, we will shortly review the OVPD® technology combined with the Close Coupled Showerhead (CCS) technology for the fabrication of sophisticated opto-electronic organic devices based on open literature. The deposition of single organic films, the morphology control by OVPD and the proposed benefits of mixing organic materials and applying non-sharp interfaces for the overall OLED performance will be discussed.

8.2 OVPD® Basics and Industrial Concept

Forrest introduced the OVPD® principle to overcome many limitations of the standard VTE [18, 19]. Due to the gas phase transport principle of OVPD® the arrangement of evaporation and condensation on a substrate is decoupled as opposed to VTE. Thus, in OVPD the evaporation area, also called source area, and deposition area can independently be optimized [16]. A schematic of *AIXTRON's* Gen 2 OVPD® equipment is shown in Fig. 8.1. The organic source materials are placed in physically separated source containers arranged in separate furnaces remote from the deposition chamber. In this example four furnaces with three source containers each are shown; however, the amount and arrangement of source containers is flexible. The temperature of each furnace, thus of the organic materials, is controlled. As a consequence a defined vapor pressure of organic material is present in the source container, which is an enclosed volume. Individual pneumatic high-temperature valves switch the source flows transporting the organic material by the carrier gas, e.g., nitrogen, towards the hot wall deposition chamber. The amount of organic material transported to the deposition area (q_{Material}), given in mol/min, is described by the formula below and depends on the vapor pressure of the organic material ($P_{\text{Vap}} = P_{\text{vap}}(T)$), the total pressure in the source container (P_{Source}), and source flow of nitrogen carrier gas through the source (q_{Source}). Here V_{mol} is the molar volume.

$$q_m = \frac{q_s}{V_{\text{mol}}} \times \frac{p_{\text{Vap}}}{p_s - p_{\text{Vap}}}$$

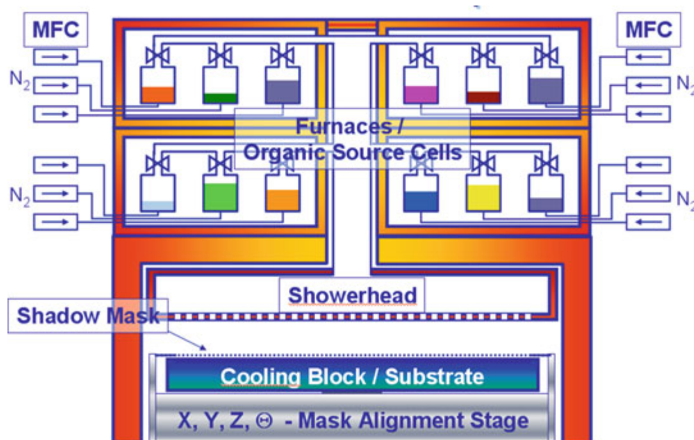

Fig. 8.1 Close Coupled Shower Head Technology for industrial scale production of organic devices by OVPD®

By altering the source flow q_{Source} using mass flow controllers (MFCs) and keeping the source temperature constant, thus P_{vap} is constant, enables a linear control of the organic material $q_{Material}$ transported to the deposition chamber [16, 18].

The individual switching of the high-temperature source valves (HT-Valves) enables a rapid on/off control of the respective deposition offering high precision control of layer interfaces as well as minimization of material waste. In addition, due to the heated runlines any unintentional condensation of organic material is avoided. The organic molecules are homogeneously mixed in the gas phase prior to be introduced uniformly through the heated showerhead across the entire substrate leading to a homogeneous condensation of the desired organic film on the substrate. The latter is placed on the cooling block and can be equipped with an alignment stage ensuring the required substrate to mask alignment. The advantages of the OVPD® technology can be fully exploited in combination with the CCS technology. The latter ensures a uniform deposition and condensation of the organic molecules over the substrate without any substrate rotation or related methods. Due to the heated lines and the controlled gas phase transport no unintended deposition of organic molecules occurs in the hot wall OVPD® chamber. Instead most of the material is deposited on the cooled substrate resulting in a high material utilization [16, 17].

This approach combining the OVPD® technology with the CCS technology enables the fabrication of a full OLED stack in a single OVPD® chamber and is not limited for scaling to any size and can be realized in a vertical or horizontal arrangement. Furthermore, this OVPD® approach for the deposition of organic films and devices offers potential for low maintenance cycles, high material yield, high reproducibility, well-defined doping with multiple dopants, films with concentration gradients and high throughput, which are key factors for industrial mass production at low cost of ownership [16, 17].

8.3 OVPD® Deposition of Organic Thin Films and Devices

8.3.1 Single Film Deposition

The basis for the fabrication of organic devices is the homogeneous deposition of high-quality, single films at high deposition rates with good controllability and reproducibility, which is important for a high tact-time and production yield. In OVPD® the source flow is precisely controlled by standard MFCs. Depending on the material specific vapor pressure the material transport can be controlled by the amount of carrier gas flow through the source. Thus, the deposition rate of each material can be adjusted as function of the source carrier flow (q_{Source}) for individual evaporation temperatures ($P_{Vap} = P_{Vap}(Temp)$) and source container pressures (P_{Source}) resulting in the expected deposition rate, as shown in Fig. 8.2 for Alq_3 deposited in a Gen1 system. With increasing source flow the Alq_3 rate increases linearly up to approximately 150 sccm followed by a sub-linear increase

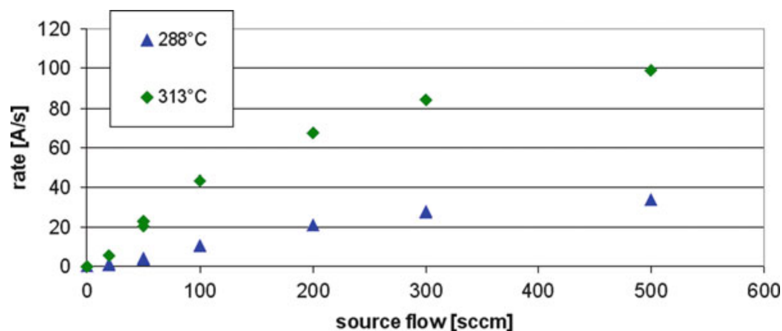

Fig. 8.2 Alq_3 rate as function of source flow with different source temperatures for a Gen1 system. The rate increases linearly with source flow up to approximately 150 sccm, followed by a sublinear increase. The rate is significantly increased with source temperature (313°C vs. 288°C) reaching 100 Å/s

towards 500 sccm. The latter is a result of the increased source container pressure P_{source} due to the higher source flow. By raising the source container temperature form 288°C to 313°C the deposition rate increases for 500 sccm up to 100 Å/s. Such high deposition rates are favorable for short tact-times. The drastic increase in rate by altered source temperature is due to the increased organic vapor pressure P_{Vap} described by the Clausius–Clapeyron equation. Worth to mention, in VTE the only option to control and increase the deposition rate is to alter the evaporation temperature. However, here a small change in source temperature has a large impact in rate. In contrast, in OVPD® the source temperature is kept at a predefined level ensuring the required range of deposition rates, but the deposition rate itself is adjusted by the nitrogen carrier gas source flow through the source container, which can be controlled in an accurate manner.

Obviously, by adding an additional source container of the same organic material at the same source temperature, the potential maximum deposition rate is doubled.

The film thickness is determined by the deposition rate and the deposition time. The latter is the time, when the source valves are open and the nitrogen carrier gas passes through the source container. The digital on/off of the HT-Valves enables the exact determination of the film thickness and sharp interfaces of subsequent organic layers. Figure 8.3 illustrates the in-situ measured Alq_3 rate for different source flows ranging from 20 sccm to 500 sccm and open (HT-Valve OPEN = 1) as well as closed source valves. With opening and closing of the source valve the in-situ measured deposition rate digitally increases and decreases, ensuring a precise control and reproducibility of the deposited film thickness. This digital on/off promotes sharp interfaces of subsequent organic layers. With increased source flow the Alq_3 deposition rate increases. Applying the same source flow the same deposition rate is achieved, obviously, as shown here for a rate of 3.9 Å/s at a source flow of 50 sccm. These results demonstrate that abrupt interfaces and reproducible thickness parameters can be realized with the control of the pneumatic source valves and precisely controlled nitrogen carrier gas flows [16, 20].

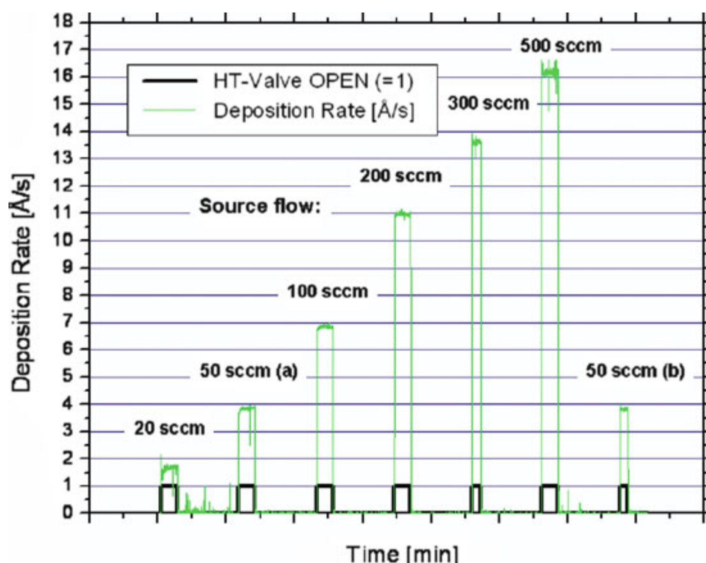

Fig. 8.3 Alq_3 deposition rate measured in-situ as function of time for different nitrogen source flows and HT-Valve switching (on/off). The Alq_3 rate shows a digital on/off and increases with source flow

In addition, not only the short-term stability but also the long-term stability of the source conditions and deposition rates was investigated in Gen1 and Gen2. For example for the latter at a rate of 12.28 Å/s a run-to-run deviation of $\sigma = 0.3\%$ was observed and over 500 h of continuous operation time at identical process parameters a standard deviation of only $\sigma = 1.93\%$ was measured [16].

The uniformity of the deposited organic films is crucial for a high production yield. OVPD® ensures by applying the CCS technology that the organic film is deposited with maximum uniformity with respect to thickness deviations over the substrate. For example for Gen1 systems thickness deviations below 2% and even below 1% were measured. In parallel for Gen2 systems an absolute thickness deviation of 1.7% over the diagonal with standard deviation $\sigma = 1\%$ were achieved [16].

These experimental uniformity values confirmed our predictions based on fluid dynamic simulations together with the material utilization efficiency for Gen2 of 50% or more. Based on these experiences the deposition chamber including showerhead was scaled and further developed towards Gen4 size ($730 \times 920\,mm^2$) and the thickness uniformity evaluated. Figure 8.4 shows the simulated deposition rate distribution over the Gen4 substrate. Here a deposition rate of 24 Å/s is shown as red color in the graph, 23 Å/s as light green and 22 Å/s as light blue color. The rates in between are interpolation from these colors. The entire Gen4 substrate shows a pure light green color illustrating that the deposition rate is very uniform over the entire substrate. The inset in the Graph shows the rate deviation assuming different edge exclusions. For a small edge exclusion of 3 mm a rate deviation of 0.52%

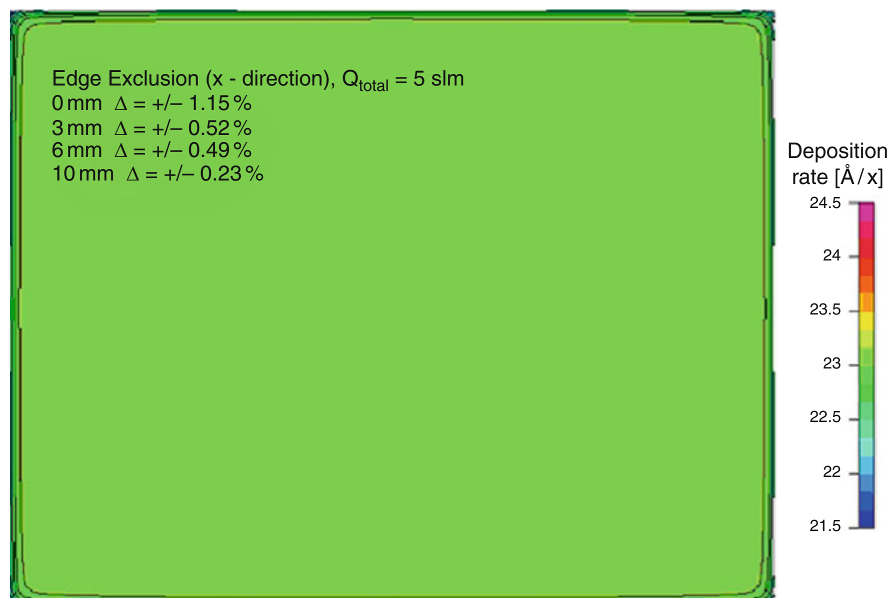

Fig. 8.4 Simulated film thickness uniformity of Alq_3 deposited on a $(730 \times 920)\,mm^2$ glass substrate

was achieved. Even in case of no edge exclusion at all (0 mm) the rate deviates only by 1.15%. This feasibility study shows that high uniformities below 2% or even below 1% can be achieved proving the good scalability of the OVPD®-CCS technology, Fig. 8.4. In addition, the material utilization efficiency is expected to increase significantly from Gen2 towards Gen4 [20].

In conclusion, we have demonstrated that the combination of CCS and OVPD® enables highly reproducible deposition rates with remarkable thickness uniformities. Extending this precise process controllability of a single material to several materials offers a valuable technology for the co-evaporation of several materials for example mixed hosts or accurate doping of dyes as will be discussed in the following.

8.3.2 Organic Film Morphology

The layer morphology, thus the physical properties, of the deposited layer are affected not only by the substrate but also by the deposition process itself and the deposition parameters, like deposition rate or substrate temperature [16, 21–23]. In VTE the source (crucible) is placed opposite the substrate. To increase the deposition rate, the crucible is heated to a higher temperature leading to higher heat radiation which passively increases the substrate temperature. Thus rate and

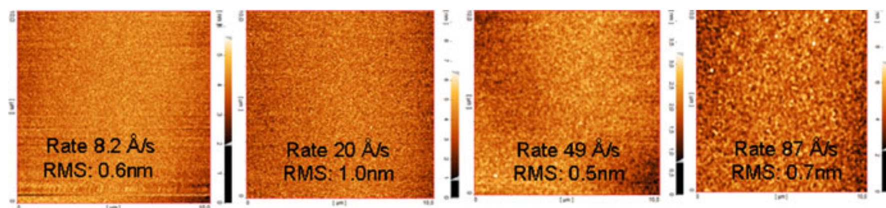

Fig. 8.5 RMS roughness of 50-nm thick α-NPD films on silicon substrates deposited with different deposition rates ranging up to 87 Å/s

substrate temperature are changed simultaneously. In contrast, in OVPD® altering the deposition rate, e.g., by changing the nitrogen source flow, has no impact on the substrate temperature due to the separation of source area and deposition area. The deposition parameters rate and substrate temperature can be altered independently [16, 17]. Furthermore OVPD® offers an additional deposition parameter, the deposition pressure, thus in total three deposition parameters to control and modify the morphology of organic films [24].

In first approximation, OLED devices require smooth films and smooth organic interfaces. To achieve a low CoO for the OLED production the tact-time should be short thus the deposition rate should be high. However, it was observed that with increased deposition rates the roughness of the deposited organic films was increased [16, 22, 23]. Thus, it is crucial to ensure that even for high deposition rates smooth organic films can be deposited. For evaluation α-NPD films with different high deposition rates ranging from 8.2 Å/s up to 87 Å/s were deposited on silicon substrates. The rates and thickness of these films were ex-situ verified by ellipsometry. The surface roughness of these 50-nm thick organic films was determined by AFM measurements and the results are shown in Fig. 8.5. The RMS-roughness of these films varies within 0.6 nm and 1.0 nm whereas the RMS value for 87 Å/s is 0.7 nm. These RMS values are in the order of the dimensions of the used organic molecules. This, proves, that even for deposition rates as high as 87 Å/s monomolecular smooth films of α-NPD were deposited, see Fig. 8.5 [25].

Whereas for OLEDs smooth interfaces are preferred the requirements for OPV cells are different. For example, to enhance the OPV efficiency the concept of a bulk heterojunction was introduced to extend the interface responsible for the electron hole splitting. As a consequence a rough morphology composed from well-defined polycrystalline or even crystalline layers are preferred instead of smooth amorphous films as preferred for OLED stacks [20,26,27]. Besides getting a rough morphology on a smooth substrate, also the planarization of a rough substrate can be an issue of interest.

Beside the topology of the organic film also the physical properties can be affected by the optimisation of the deposition parameters. Figure 8.6 shows the measured current density for a hole-only-device as function of the substrate temperature during deposition of the HIL material. Increasing the substrate temperature towards 40°C results in a significant increase of the current density

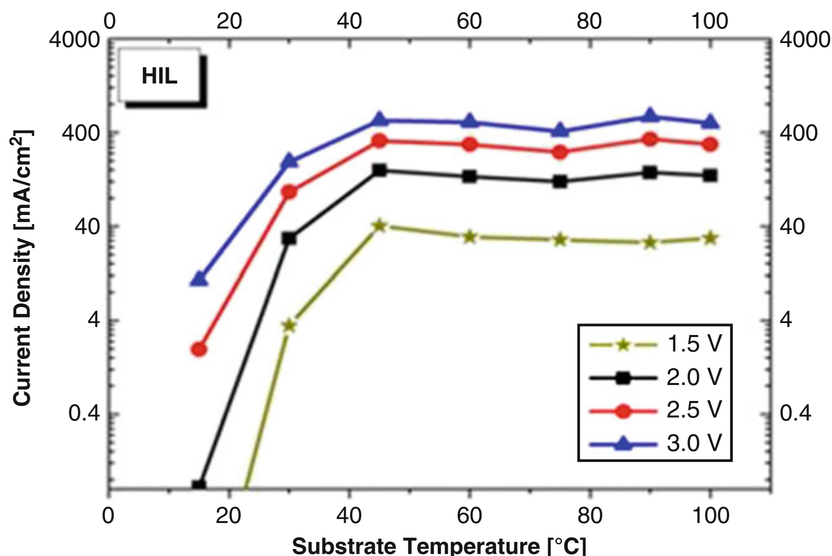

Fig. 8.6 Current density of a hole-only-device based on a material for a hole injection layer (HIL). When deposited at higher substrate temperature the current density improves

improving the electrical conductivity of the investigated HIL material [25]. This demonstrates, that the potential of an organic material, which shows, e.g., at the first investigation no promising material properties, can be fully exploited by optimizing the deposition parameters. This parameter optimisation is obviously not limited to the substrate temperature but also the deposition pressure or rate could be used for optimisation.

Typically the used organic materials offer a broad deposition parameter window with respect to rate, substrate temperature, and pressure for the deposition of smooth films. However, some organic film and material properties might by possible to be improved with respect to the device and production requirements. This is especially true for OPV application, where rough and even crystalline films are preferred for some applications. It can be concluded that OVPD® offers the option to achieve specific organic film morphologies required by individual process parameters.

8.3.3 OLED Stack Designs Fabricated by OVPD® – Cross-Fading

Research on organic semiconductor materials has shown remarkable progress with the introduction of material combinations using hosts and single or multiple guests or additional host materials [9, 13, 28]. In the previous chapter we have explained

the OVPD® process parameters, which are essential for the deposition of single layers. Applying this concept of precise source flow controllability and long-term source stability to additional sources enables precise deposition, co-deposition, and doping of multi-component layers. In general, doping ranges from 0.1 to 50% are of interest in actual device development which can be processed by OVPD® [16]. Besides this huge doping range the standard MFC guarantees an accurate and reproducible controllability for the deposition of single layers and even allows a dynamic variation of each individual source flow. OVPD® uses physically separated sources such that organic material transport can be extended from a single source to a high number of sources leading consequently to the deposition of any mixtures or doped layers, known as co-evaporation or co-hosting. For example, the deposition of an OLED stack with an EML consisting of a host and two dopants, a red and a green dye molecule. Here the controllability and reproducibility of the OVPD® process is proven by the reproduction of layer composition even for a red dopant concentration of 0.26% and reproduced emission spectrum of the OLED [20].

By controlling the organic flux of two or even more organic materials the concentration of each organic species can be homogenously adjusted to any desired ratio in an abrupt or a ramping mode offering the potential to create precise constant mixtures or mixtures with a gradual concentration within the layer [16]. Figure 8.7 gives an overview of different potential constant or gradual material mixtures controlled by the deposition rates of, e.g., three materials (r_1, r_2, and r_3). The organic materials are mixed in the gas phase and homogeneously deposited over the substrate due to the CCS technology.

In zone 1, the source flow of materials 1 and 2 is switched on and the total deposition rate is the sum of both individual rates ($r_{tot} = r_1 + r_2$). In zone 2, the

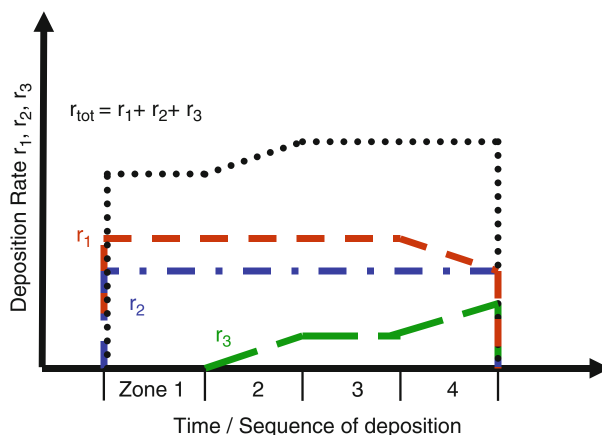

Fig. 8.7 Each zone represents a schematic material mixture based on three organic materials. Zone 1 is a mixture of the materials 1 and 2 and zone 3 of the materials 1 and 2 and 3. In zone 2 the rate r_3 of the material 3 is ramped leading to a concentration gradient. Whereas in zone 4 the rate r_1 is reduced and simultaneously the rate r_3 increased which is described as layer cross-fading [29]

Fig. 8.8 Reference OLED structure with phosphorescent red dopant [29]

LiF / Al		
30 nm	ETL	ETM001
40 nm	EML	H001:G001 (7 %)
20 nm	HTL	HTM001
20 nm	HIL	HIM001
ITO		

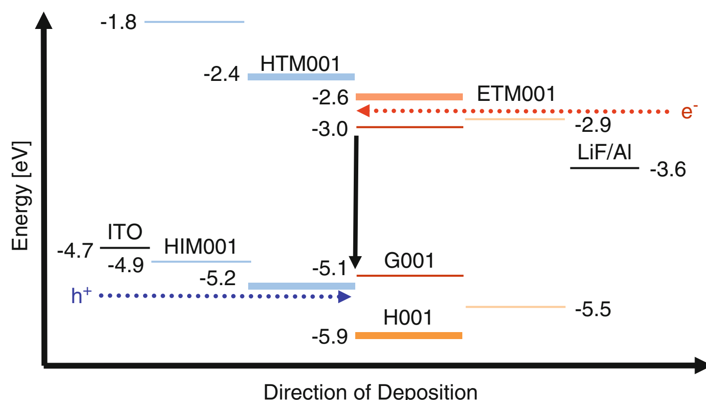

Fig. 8.9 HOMO and LUMO schematic for the reference red OLED, here without the CFL layer. The electrons are injected from the ETL towards the EML and the holes from the HIL via HTL towards the EML. At the interface HTL to EML a charge accumulation occurs [29]

rate of material 3 is increased linearly increasing the total deposition rate ($r_{tot} = r_1 + r_2 + r_3$) and simultaneously the concentration of material 3 in the deposited layer. This leads to a concentration gradient. In zone 3, a constant mixture of the materials 1 and 2 and 3 is deposited. In zone 4, the deposition rate of material 2 is kept constant, whereas material 1 is linearly "faded out" and rate of material 3 is increased with the opposite slope. This special version of a concentration gradient is an example for cross-fading.

The benefit of a concentration gradient on the device performance was already reported either for OLEDs [15, 30] or for OPV fabricated by OVPD® [26]. How the concept of cross-fading can be applied to an organic device and enables a new parameter of freedom for the overall stack and design and will be demonstrated in the following [25, 30–32]. Figure 8.8 shows a reference red OLED stack with 40 nm EML and 20 nm HTL which serves as reference for this investigation. The corresponding HOMO and LUMO levels are given in Fig. 8.9. Due to the gap in the HOMO levels at the HTL to EML interface a charge accumulation is present which is especially relevant at larger currents leading to the well-known roll-off-effect, which is a reduction of the current efficacy as function of the luminance [25, 31].

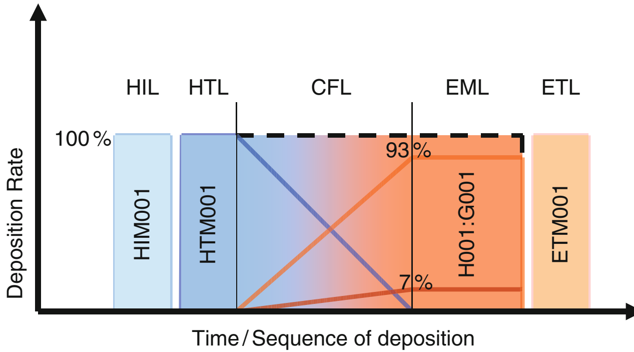

Fig. 8.10 Reference red OLED stack with additional cross-fading layer (CFL) between HTL and EML. The total thickness of HTL+CFL+EML was kept constant with 60 nm [29]

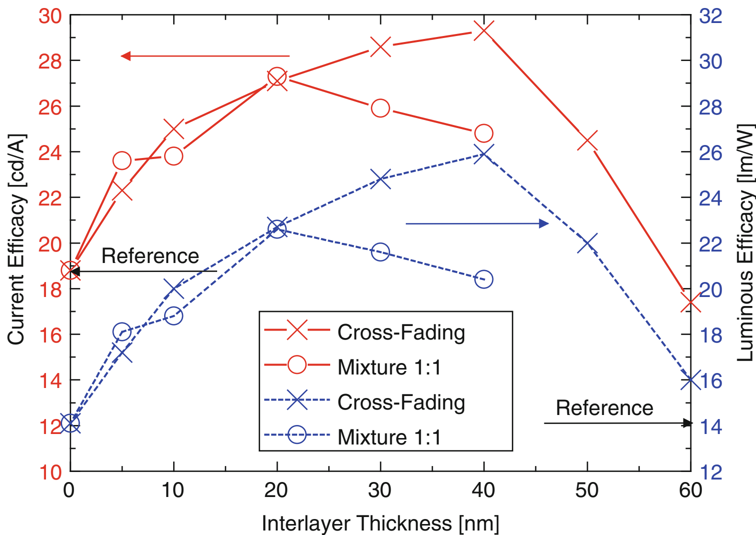

Fig. 8.11 Current and luminous efficacy vs. thickness of CFL and constant mixture interlayers [29]

The cross-fading concept was applied for the red reference OLED by introduction of an additional cross-fading layer (CFL) between HTL and EML as illustrated in Fig. 8.10 [25, 29, 31]. In the CFL is the rate of the hole transport material (HTM001) linearly reduced towards zero whereas the rate of the Host material (H001) and of the red guest respectively red dopant (G001) are linearly increased starting from zero. The total thickness of HTL+CFL+EML was 60 nm and kept constant throughout these experiments. In addition and for comparison a structure with an interlayer between HTL and EML with constant ratio of 1:1 for the HTM001 and H001 were also investigated. The impact of the CFL layer with varying thickness between HTL and EML on the OLED performance is shown in Fig. 8.11 [29].

For this investigation, the reference phosphorescent red OLED device had at 1,000 nits a luminous efficacy of 14.1 lm/W and a current efficacy of 18.8 cd/A at 4.18 V [25, 29, 31]. The color point of all investigated OLEDs either with or without CFL is the same with CIE (0.62/0.38). The motivation for the cross-fading approach is the reduction of charge carrier accumulation at the interface of HTL to EML and a broadening of the recombination zone at higher current densities, thus an improved carrier distribution in the EML. Thus, at the interface HTL to EML an additional layer will be introduced consisting either of a constant mixture of the neighboring organic materials or a cross-fading composition, as illustrated in Fig. 8.10. To ensure an objective judgment and comparison on the achieved the total thickness of HTL+CFL+EML was kept with 60 nm the same as for the reference red OLED stack, see Fig. 8.8. Figure 8.11 shows the measured current efficacy (left axis) and luminous efficacy (right axis) vs. the interlayer thickness in comparison of devices utilizing cross-fading (red) and layers with constant mixing ratio (blue). Increasing the interlayer thickness improves for the layer with a 1:1 mixture as well as for the CFL structure the current efficacy as well as the luminous efficacy. However, at an interlayer thickness of 20 nm the efficacy for the mixture structure reaches its maximum and decreases with increasing interlayer thickness. In contrast the efficacy for the CFL structure improves further. The maximum efficacy is achieved at a CFL thickness of 40 nm with a current efficacy of 29.3 cd/A and luminous efficacy of 25.9 lm/W [25, 29, 31]. Thus, by using the CFL concept the luminous efficacy could be improved by 139% compared to the reference OLED. The increase in efficacy is attributed to an improved hole injection from the HTL to EML suppressing charge accumulation due to the lower HOMO level of the H001 compared to the HTM001. In addition, cross-fading of the predominately hole conducting zone with the predominately electron conducting zone enables a interpenetrating molecular network resulting in a broadening of the recombination zone, especially a higher current densities [29, 31]. As a consequence, the roll-off effect improves due to the CFL approach [25, 31]. Further increase of the CFL thickness beyond 40 nm results in decreasing efficacies attributed to a shift of the recombination zone. It can be concluded that the introduction of an interlayer with a mixture and even with a cross-fading concept are options to enhance the overall device performances [25, 29, 31, 33].

In the above example, an additional CFL was introduced. However, the cross-fading concept can be extended to the EML design itself. Additional optimisation of the red OLED stack lead to 34 lm/W and an EQE of 18% without applying no ILO techniques [29]. Furthermore, the concept of cross-fading can be extended even to an OLED stack with two or more optical dopants. For example, using a phosphorescent green and red dopant in a cross-faded EML enables an efficient and easy adjustable OLED emission ranging from red via yellow towards green [32]. The concept of creating a virtual host material by mixing a predominately hole conducting host with a predominately electron conducting host creating a host with locally preferential electrical properties. This leads to an efficient carrier balancing in the emission zone. Nearly luminance independent CIE coordinates were observed and the external quantum efficacy (EQE) was 16.2%, the luminous

efficacy 32.8 lm/W and the current efficacy 36.5 cd/A at 1,000 nits. Applying an EML with a constant mixture of the two host materials does not achieve such results [32]. The limiting factor for the EQE is likely related to the applied phosphorescent green dopant. Further improvements on the yellow OLED stack by improved cross-fading are promising. Thus, the cross-fading concept truly is a measure to improve the OLED performance of monochrome but also mixed OLEDs.

In summary, the realization of vertical doping profiles like simple gradients or CFLs and multi-material mixtures allow a precise layer fine-tuning to optimize device performance. Here, OVPD® combined with the CCS technology offers the ability to fabricate such kind of OLED stacks either in R&D or production and this with high uniformity and further benefits offered by the OVPD® technology.

8.4 Conclusion

The OVPD® technology uses a carrier gas to transport the evaporated organic materials from the source area towards the substrate. This is in contrast to the VTE technology. Beside the pure deposition of the organic film also the morphology and physical properties are crucial, which can be altered and controlled by the OVPD® deposition parameters rate, substrate temperature, and process pressure. A detailed comparison of the OVPD® technology with the VTE technology is given elsewhere [16]. OVPD® combines the individual control of deposition rate of organic materials, their homogenous mixing in the gas phase and deposition as film on the substrate with the option of multi-layer deposition with different layer compositions and even complex concentration gradients like cross-fading. Applying the cross-fading concept to monochrome and multicolor OLED shows significant improvements in the device performance. Thus, in parallel to the replacement of MBE by MOCVD the OVPD® technology has the potential to overcome the limitation of VTE.

Acknowledgments This work was the result of a team effort from the groups at AIXTRON AG, Philips BU OLED, Aachen, Technische Hochschule (TU) Braunschweig, and the Rheinisch Westfälische Technische Hochschule (RWTH), Aachen, which performed most of the work reported in this article.

Part of this work was financially supported by the Federal Ministry of Education and Research in Germany (BMBF, No. 001BD153; No. 13N8650, No. 13N8993, and BMU 0329927B).

OVPD® technology has been exclusively licensed to *AIXTRON* from *Universal Display Corporation*, Ewing, NJ, USA, for equipment manufacture. OVPD® technology is based on an invention by Professor Stephen R. Forrest et al. at Princeton University, USA, which was exclusively licensed to UDC, AIXTRON, and UDC have jointly developed and qualified OVPD® pre-production equipment.

References

1. C.W. Tang, S.A. VanSlyke, Appl. Phys. Lett. **51**, 913 (1987)
2. L.S. Hung, C.H. Chen, Mater. Sci. Eng. **R 39**, 143 (2000)
3. S.R. Forrest, Chem. Rev. **97**, 1793 (1997)
4. S.R. Forrest, MRS Bull. **30**, 28 (2005)
5. B.D'Andrade, V. Adamovich, R. Hewitt, M. Hack, J.J. Brown, SPIE **5937**, 87 (2005)
6. J. Shinar, *Organic Light-Emitting Devices: A Survey*, (Springer, New York, USA, 2004)
7. http://www.lumiblade.com; http://www.osram-os.com
8. J. Kido, M. Kimura, K. Nagai, Science **267**, 1332–1334 (1995)
9. M. Hack, *International Summer School on OLEDs, Organic Electronics: from Lab to Home*, Krutyn, Poland, 2–8 June 2009; Organised by oled100.eu
10. http://www.universaldisplay.com
11. S. Reineke, F. Lindner, G. Schwartz, N. Seidler, K. Walzer, B. Lüssem, K. Leo, Nature **459**, 08003 (2009)
12. H. Kanno, Y. Hamada, N. Matsusue, H. Takahashi, R. Nishikawa, K. Mameno, *SPIE Conference on Organic Light-Emitting Materials and Devices VII*; San Diego, California, USA, 4–6 Aug 2003
13. B.W. D'Andrade, J.Y. Tsai, C. Lin, M.S. Weaver, P.B. Mackenzie, J.J. Brown, *SID 2007* (Long Beach, CA, USA, 20–25 May 2007)
14. N. Meyer, M. Rusu, S. Wiesner, S. Hartmann, D. Keiper, M. Schwambera, M. Gersdorff, M. Kunat, M. Heuken, W. Kowalsky, M.C.h. Lux-Steiner, Eur. Phys. J. Appl. Phys. **46**, 12506 (2009)
15. J. Kido, *Plastic Electronic 2007* (Frankfurt, Germany, **7**.10.n2007)
16. N. Meyer, M. Heuken, *Review About Organic Vapor Phase Deposition for Organic Electronics,* ed. by H. Klauk (Wiley-VCH, Weinheim, Germany, 2006) ISBN: 9783527312641, pp. 203–232
17. B. Marheineke, SPIE Proc. **5961**, 3 (2005)
18. M. Shtein, H.F. Gossenberger, J.B. Benzinger, S.R. Forrest, J. Appl. Phys. **89**(2), 1470 (2001)
19. P.E. Burrows, S.R. Forrest, L.S. Sapochak, J. Schwartz, P. Fenter, T. Buma, V.S. Ban J.L. Forrest, J. Crystal Growth, **156**, 91 (1995)
20. N. Meyer, M. Rusu, S. Wiesner, S. Hartmann, D. Keiper, M. Schwambera, M. Gersdorff, M. Kunat, M. Heuken, W. Kowalsky, M.C.h. Lux-Steiner, Eur. Phys. J. Appl. Phys. **46**(1), 12506, (2009)
21. T. Kato, T. Mori, T. Mizutani, Thin Solid Films **393**, 109 (2001)
22. F. Yang, M. Shtein, S.R. Forrest, J. Appl. Phys. **98**, 014906 (2005)
23. S.Y. Yang, K. Shin, C.E. Park, Adv. Funct. Mater. **15**, 1806–1814 (2005)
24. P. Niyamakom, Phd thesis, RWTH, Aachen, Germany, 2008
25. Project report. Förderkennzeichen BMBF 13N8993 (2009) http://edok01.tib.uni-hannover.de/edoks/e01fb09/610461389l.pdf
26. M. Rusu, J. Gasiorowski, S. Wiesner, D. Keiper, N. Meyer, M. Heuken, K. Fostiropoulos, M.C.h. Lux-Steiner, *EMRS Conference*, Strasbourg, France, 26–30 May 2008
27. M. Rusu, J. Gasiorowski, S. Wiesner, D. Keiper, N. Meyer, M. Heuken, K. Fostiropoulos, M.C.h. Lux-Steiner, (2008): 23rd EUPVSEC, Valencia, Spain, 1–5 September, 2008: WIP-Renewable Energies, ISBN: 3–936338–24–8, pp. 679–681
28. H. Hoppe, N.S. Sariciftci, J. Mater. Res. **19**(7), 1924–1945 (2004)
29. C. Himcinschi, S. Hartmann, A. Janssen, N. Meyer, M. Friedrich, W. Kowalsky, D.R.T. Zahn, M. Heuken, J. Cryst. Growth **275**, e1035 (2005)
30. M. Schwambera, D. Keiper, N. Meyer, M. Heuken, F. Lindla, M. Bösing, C. Zimmermann, F. Jessen, H. Kalisch, R.H. Jansen, P.v. Gemmern, D. Bertram, IMID 2009, KINEX Seoul, Korea, 13–15 October 2009

31. M. Bösing, C. Zimmermann, F. Lindla, F. Jessen, P. van Gemmern, D. Bertram, D. Keiper, N. Meyer, M. Heuken, H. Kalisch, R.H. Jansen, 2009 *Material Research Society (MRS) Spring eeting*, San Francisco, CA, USA, 13–17 April 2009
32. F. Lindla, M. Bösing, C. Zimmermann, F. Jessen, P. van Gemmern, D. Bertram, D. Keiper, N. Meyer, M. Heuken, H. Kalisch, R.H. Jansen, *Material Research Society (MRS) Spring Meeting*, (San Francisco, CA, USA, 13–17 April 2009)
33. F. Lindla, M. Bösing, C. Zimmermann, F. Jessen, P. van Gemmern, D. Bertram, D. Keiper, N. Meyer, M. Heuken, H. Kalisch, R.H. Jansen, Appl. Phys. Lett., **95**, 213305 (2009)